Research on Optimizing the Partition Plate Design for the Super-tall Piers of Partial Cable-stayed Bridges in Mountainous Areas

Shaohui Xiong[1, 3,a], Lu Kuang[2,b], Xuefeng Dou[2,c], Zuoqiao You[1, 3,d*], Chaojie Miao[2, e]

[1]China Merchants Chongqing Communications Technology Research & Design Institute Co., Ltd., Chongqing, 400067, China
[2]Chongqing Yuxiang Double-line Expressway Co., Ltd., Chongqing, 408599, China
[3]State Key Laboratory of Bridge Safety and Resilience, Chongqing, 400067, China

[a]381234694@qq.com, [b]609717361@qq.com, [c]490863038@qq.com
[d*]youzuoqiao@foxmail.com, [e]874098896@qq.com

Abstract. Due to the topographical constraints in mountainous areas, hollow thin-walled high piers are typically employed for highway bridges. To enhance the stability of these high piers, both transverse and vertical diaphragms are usually installed, which, however, increases construction difficulty and reduces efficiency. To address this issue, this study investigates the impact of transverse and vertical diaphragm placement on the stability of hollow thin-walled high piers. Using Midas Civil and Midas FEA finite element software, the study examines a low-tower cable-stayed bridge currently under construction. The analysis focuses on the internal forces at the pier top and the effects of wind load during the maximum cantilever stage. The results indicate that transverse diaphragms have a minimal effect on the overall stability of hollow thin-walled piers, primarily affecting local stability. Therefore, reducing the number of transverse diaphragms can facilitate construction. Similarly, vertical diaphragms also have a minimal effect on the overall stability, mainly influencing local stability. Increasing the wall thickness can enhance the overall stability of the piers.

Keywords: partial cable stayed bridge, super high pier, diaphragm, mediastinal plate, stability.

1 Introduction

Mountain highways, due to topographical constraints, typically require tall piers and long-span bridges to cross rivers, gorges, and other complex terrains [1]. Thin-walled high piers are better suited to the complex topography, geological features, navigation, and route requirements of mountainous areas, and thus are widely used in practical engineering [2]. For some cable-stayed bridges with ultra-high piers in mountainous regions, the main pier type is single-leg hollow thin-walled piers. This type of pier has excellent torsional performance and good overall structural stability when the main

F. Ding et al. (eds.), *Proceedings of the 2024 International Conference on Civil Engineering Structures and Concrete Materials (CESCM 2024)*, Advances in Engineering Research 247,
https://doi.org/10.2991/978-94-6463-564-5_11

girder is constructed using the cantilever casting method. It is also convenient and efficient to construct [3-5]. However, in practical engineering, hollow thin-walled high piers include not only horizontal diaphragms but also vertical diaphragms. The presence of horizontal and vertical diaphragms increases construction difficulty and reduces efficiency. Therefore, to address this issue, it is necessary to simultaneously consider the impact of horizontal and vertical diaphragms on the stability of hollow thin-walled high piers.

The main span arrangement of the Mozhai Wujiang Grand Bridge is 153m+296m+153m, with the superstructure being a low-pylon cable-stayed bridge in a continuous rigid frame system. The main piers are single-leg hollow thin-walled piers, with pier 3 being 216m tall and pier 4 being 185m tall. Both the main span length and the height of pier 3 are world records. The pier body has a significant thickness, with the minimum thin-walled thickness being 1.3m and the maximum thickness being 1.8m. The piers are equipped with multiple layers of horizontal diaphragms and vertical diaphragms of varying heights. The horizontal diaphragm thickness is 2m, while the vertical diaphragm thickness ranges from 0.6m to 0.8m. The sectional structure of the piers is shown in Fig. 1. Therefore, this paper studies the impact of horizontal and vertical diaphragm configurations on the stability of ultra-high piers based on the characteristics of the high piers of this bridge. The study results are used to optimize the diaphragm configurations, aiming to simplify the structure of hollow thin-walled piers, facilitate construction, and save materials. The research results can provide a reference for the optimization design of similar high-pier bridge structures.

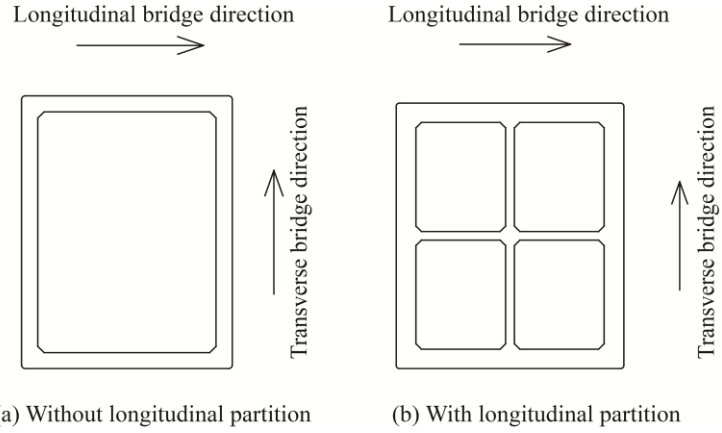

Fig. 1. Structural drawing of pier section of Mozhai Wujiang super large bridge

2 Construction of Finite Element Model

2.1 Calculated Load

The Mozhai Wujiang Grand Bridge is constructed using the cantilever casting method. During the maximum cantilever stage of the main girder construction, the structure

faces significant stress with minimal constraints, resulting in poor stability at this stage. Therefore, in the design of the main pier, the state during the maximum cantilever stage is generally used as the control point for stability [6,7]. At this stage, the loads on the structure primarily include self-weight, prestress, cable tension, wind load, and construction load. In this study, the Midas Civil finite element software was used to establish a full-bridge finite element model, and the internal force data at the top of pier 3 was extracted for the maximum cantilever stage of the main girder construction. The finite element model for the maximum cantilever stage is shown in Fig. 2, and the corresponding internal force data at the top of the pier is summarized in Table 1. It should be noted that the internal force data at the top of the pier does not consider the effect of wind load; this effect will be considered in subsequent analyses using the Midas FEA solid model of the pier [8,9]. According to the relevant calculation requirements of the "Wind resistant Design Specification for Highway Bridges" (JTG/T 3360-01-2018), the wind load q in the longitudinal direction of the bridge is 1.218 kN/m^2. In the Midas FEA bridge pier solid model, the wind load is loaded in the form of uniformly distributed surface load.

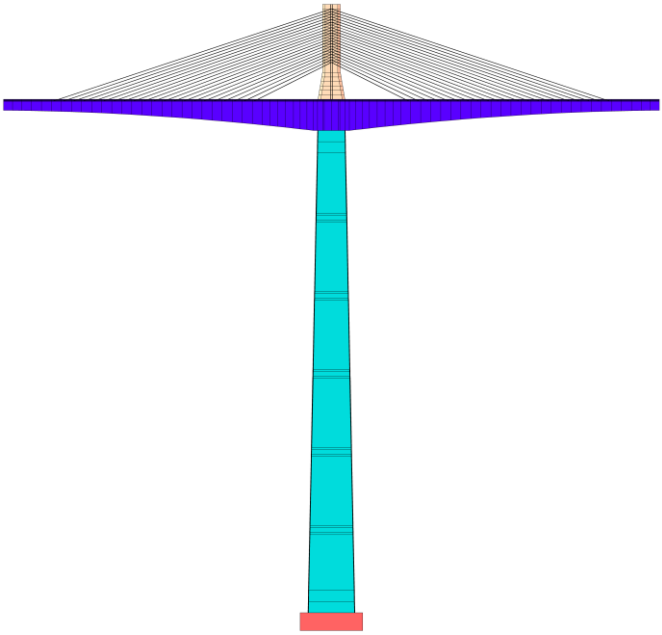

Fig. 2. Finite element model of maximum cantilever stage

Table 1. Pier top internal force at maximum cantilever stage

Axial force F_N	Bending moment M_y	Shear force F_Q
kN	kN·m	kN
4.823×10^5	1.208×10^4	1.821×10^3

2.2 Calculation Model

To enhance computational efficiency and facilitate mesh division, the Midas FEA solid finite element model of a hollow thin-walled high pier is moderately simplified without compromising the analysis results [10,11]: (1) Given the complexity of the actual pier's reinforcement layout, the impact of reinforcement on the pier's stability is conservatively ignored; (2) To facilitate mesh division, the pier's manhole and chamfered sections are disregarded; (3) The maximum cantilever phase of the main beam is simplified as an internal force acting on the centroid of the pier top, while the longitudinal wind load on the pier body is applied to the solid finite element model as a uniformly distributed surface load [12]. The schematic of the most unfavorable loading on the high pier is depicted in Fig. 3.

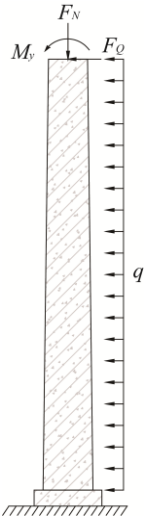

Fig. 3. Schematic diagram of model loading

Given the favorable geological conditions of the pier foundation and its use of a pile cap foundation, the study does not account for elastic foundation effects. Therefore, the calculation model assumes the bottom of the pier to be fixed while the top remains free [13,14]. The bearing platform, diaphragms, pier walls, and solid concrete sections are all modeled using 3D elements [15]. With the exception of the bearing platform, which is constructed of C45 concrete, all other components are built with C50 concrete.

3 Linear Buckling Analysis

3.1 Influence of Diaphragm on Pier Stability

To investigate the impact of diaphragms on the stability of hollow, thin-walled high piers, six scenarios were developed and designated as HG-1, HG-2, HG-3, HG-4, HG-5, and HG-6. Detailed scenarios can be found in Table 2 and Fig. 4.

Table 2. Working condition description of diaphragm

Working condition	Describe
HG-1	Original design
HG-2	No diaphragm
HG-3	The third diaphragm originally designed
HG-4	The second and fourth diaphragms originally designed
HG-5	The first, third and fifth diaphragms of the original design
HG-6	The first, second, fourth and fifth diaphragms in the original design

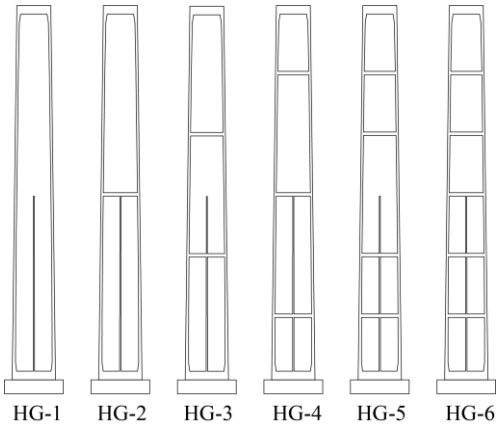

Fig. 4. Cross section of diaphragm pier

Based on Table 2 and Fig. 4, by altering the arrangement of the transverse diaphragms while maintaining the layout of the longitudinal diaphragms in the hollow thin-walled piers, a linear buckling analysis is conducted for the piers under six different conditions. This yields the eigenvalues and buckling modes for the first five buckling modes. Detailed results are illustrated in Fig. 5.

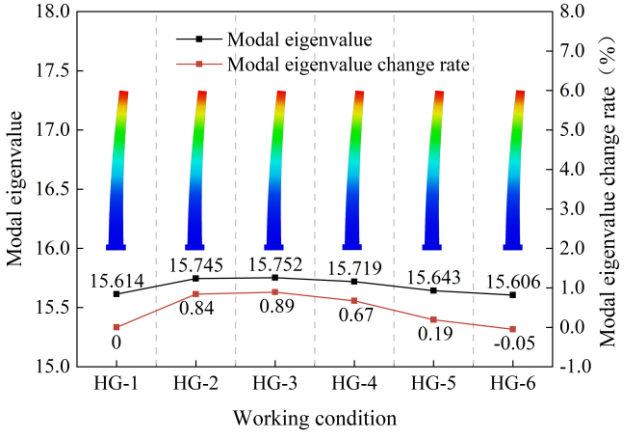

(a) First order buckling modal analysis results

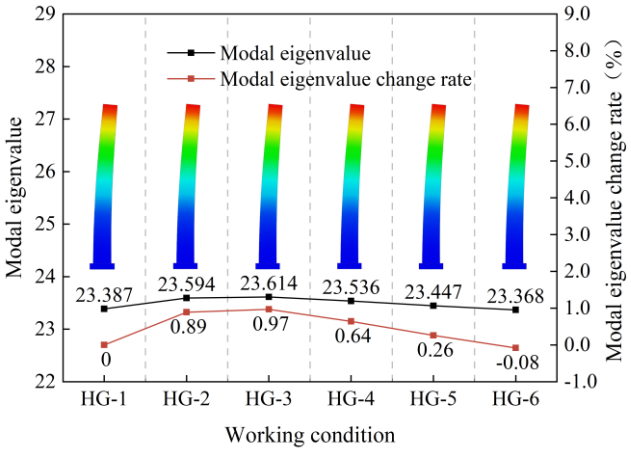

(b) Second order buckling modal analysis results

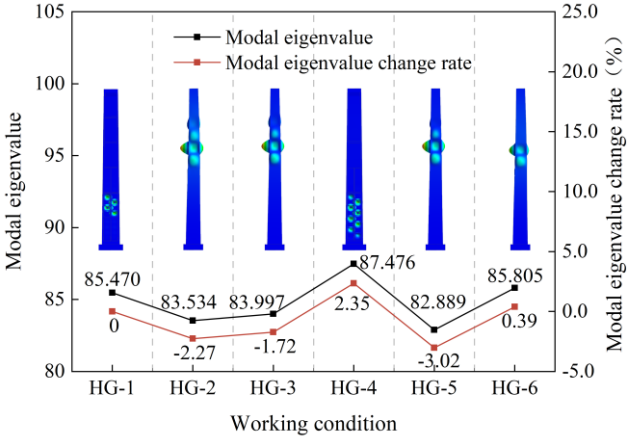

(c) Third order buckling modal analysis results

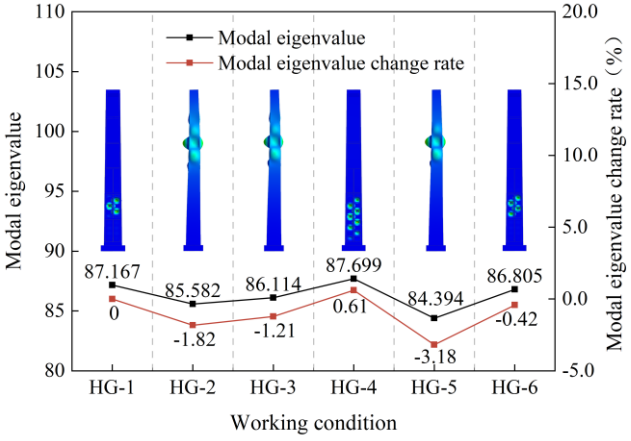

(d) Fourth order buckling modal analysis results

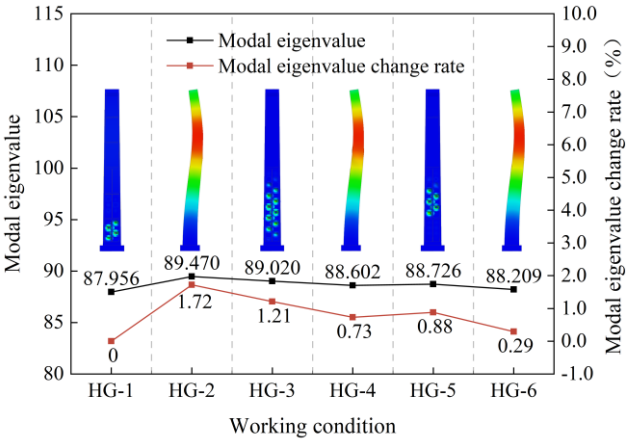

(e) Fifth order buckling modal analysis results

Fig. 5. Modal eigenvalues and rate of change

From Fig. 5, it can be observed that the first-order and second-order buckling modes of the pier under six different diaphragm conditions both exhibit overall instability, with the HG-3 condition having the highest modal characteristic value. Compared to the modal characteristic value of the original design HG-1 condition, the variation rates of the first-order and second-order modal characteristic values of the HG-3 condition are 0.89% and 0.97%, respectively, both of which are less than 1%. This indicates that diaphragms have a minimal impact on the overall stability of hollow thin-walled piers. According to the third-order and fourth-order buckling modes, it can be seen that the piers mainly exhibit local instability under each condition, suggesting that diaphragms primarily affect the local stability of the piers. For the fifth-order buckling mode, HG-1, HG-3, and HG-5 conditions exhibit local instability of longitudinal diaphragms, while HG-2, HG-4, and HG-6 conditions exhibit second-order instability along the bridge direction. Additionally, the modal characteristic values for HG-2 to HG-6 conditions are all greater than that of the original design HG-1 condition. In practical engineering, higher-order modes are usually not considered; the first-order modal characteristic value most accurately represents the critical load for pier instability. Therefore, diaphragms do not play a decisive role in the overall stability of this pier. Taking into account the modal characteristic values, construction costs, and other factors, it is feasible to consider removing some diaphragms and adopting the diaphragm arrangement of the HG-3 condition for this pier.

3.2 Influence of Mediastinal Plate on Pier Stability

To investigate the impact of longitudinal diaphragms on the stability of hollow thin-walled high piers, six different conditions were designed, named ZG-1, ZG-2, ZG-3, ZG-4, ZG-5, and ZG-6. The specific conditions are detailed in Table 3 and illustrated in Fig. 6.

Table 3. Working condition description of longitudinal diaphragm

Working condition	Describe
ZG-1	Original design
ZG-2	Set up a mediastinal plate between the pier bottom and the pier top
ZG-3	Set a mediastinal plate between the pier bottom and the second diaphragm
ZG-4	Set a mediastinal plate between the pier bottom and the first diaphragm
ZG-5	No mediastinum
ZG-6	No mediastinal plate is set, but the thickness of the mediastinal plate is assigned to the wall thickness

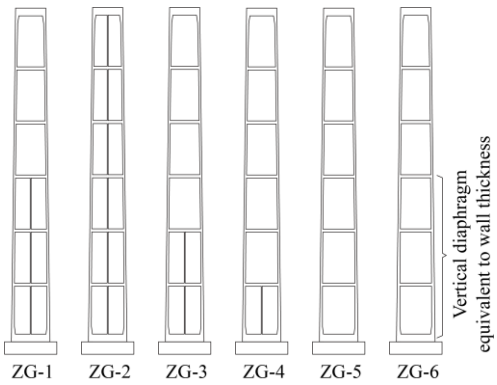

Fig. 6. Schematic diagram of section of bridge pier with mediastinal slab

From Table 3 and Fig. 6, it can be seen that the arrangement of the transverse diaphragms in the hollow thin-walled piers remains unchanged, while the arrangement of the longitudinal diaphragms varies. A linear buckling analysis was conducted on the piers under the six different conditions, yielding the first five orders of buckling modal characteristic values and buckling modes. The specific results are presented in Fig. 7.

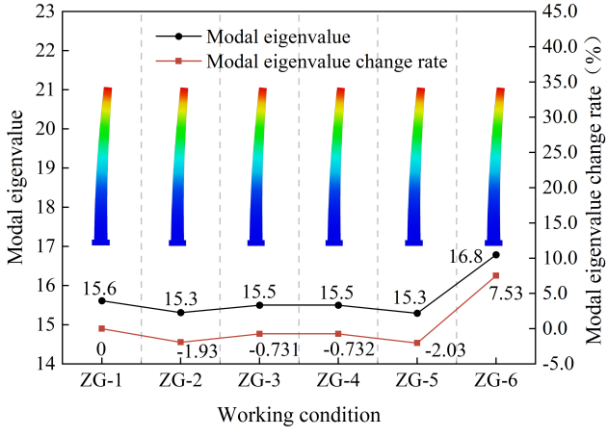

(a) First order buckling modal analysis results

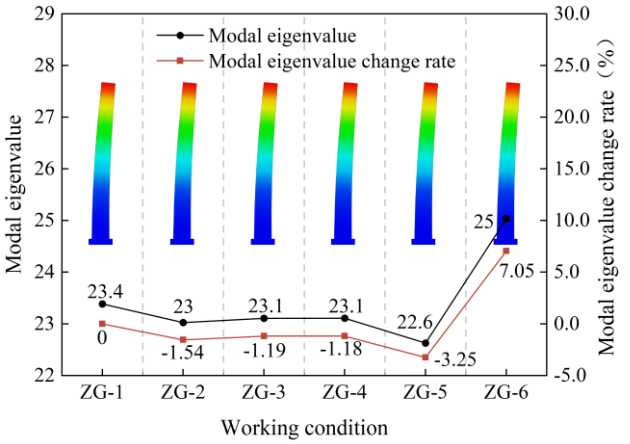

(b) Second order buckling modal analysis results

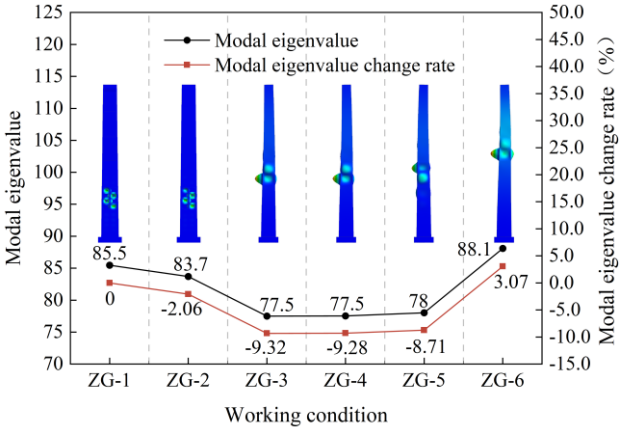

(c) Third order buckling modal analysis results

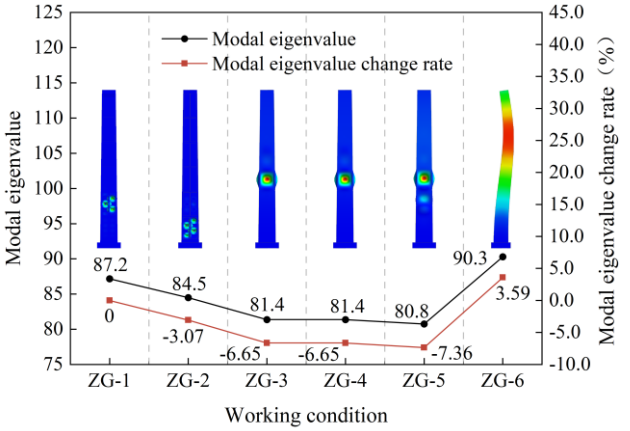

(d) Fourth order buckling modal analysis results

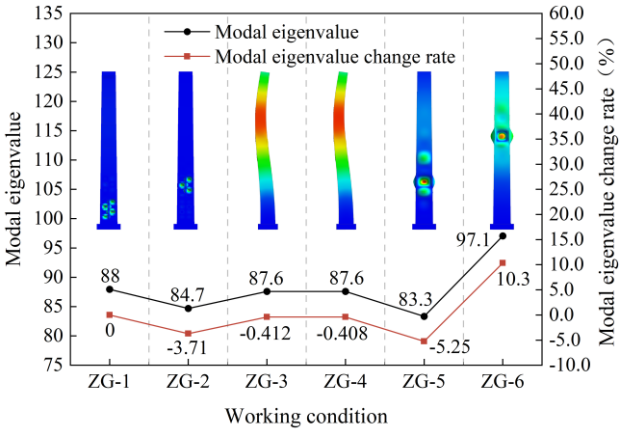

(e) Fifth order buckling modal analysis results

Fig. 7. Modal eigenvalues and change rate

According to Fig. 7, the first and second buckling modes of the six longitudinal baffle conditions for the pier exhibit overall instability. The eigenvalues of the first modes are 15.6, 15.3, 15.5, 15.5, 15.3, and 16.8, respectively. Compared to the original design condition ZG-1, the rate of change in the eigenvalues of the first mode for the other conditions are -1.93%, -0.731%, -0.732%, -2.03%, and 7.53%. It can be seen that the longitudinal baffles have a relatively minor impact on the overall stability of the hollow thin-walled pier, but assigning the thickness of the longitudinal baffles to the wall thickness can improve the overall stability of the pier. According to the third buckling mode, it can be observed that ZG-1 and ZG-2 both exhibit local instability between the first and second horizontal baffles, while the remaining conditions show local instability in the pier walls. This indicates that setting longitudinal baffles can effectively improve the local stability of the pier. For piers with reduced longitudinal baffles, the eigenvalues of each mode are relatively large. In practical engineering, the eigenvalue of the first mode best represents the critical load at which the pier becomes unstable. Therefore, longitudinal baffles do not play a decisive role in the overall stability of this pier. Comparing the ZG-1 and ZG-6 conditions, it is found that the eigenvalues of the first to fifth modes of the ZG-6 condition are greater than those of ZG-1. This demonstrates that assigning the thickness of longitudinal baffles to the wall thickness can more effectively improve the stability characteristics of the pier than directly setting longitudinal baffles. Therefore, considering the eigenvalues of buckling modes, construction costs, and construction factors, this pier can consider either eliminating longitudinal baffles or using the HG-6 condition to assign the thickness of longitudinal baffles to the wall thickness to enhance both the overall and local stability of the pier.

3.3 Influence of Vertical and Horizontal Diaphragms on Pier Stability

Based on the stability analysis results of the transverse and longitudinal baffles mentioned earlier, an optimized pier baffle model can be derived. In this optimized model,

based on the original design, only one transverse baffle is installed, and the thickness of the longitudinal baffles is added to the pier wall thickness. The optimized pier model under the new conditions is shown in Fig. 8.

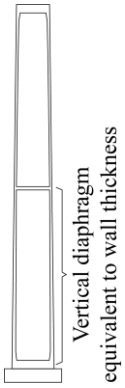

Fig. 8. Schematic diagram of optimized pier model

For both the original design condition and the optimized condition, linear buckling analysis was conducted on the piers, and the results for the first five buckling mode eigenvalues and mode shapes are presented in Fig. 9.

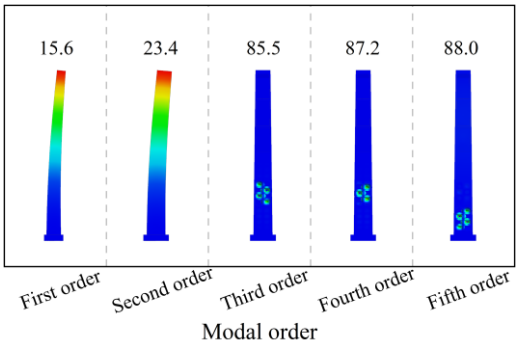

(a) Buckling mode under original design condition

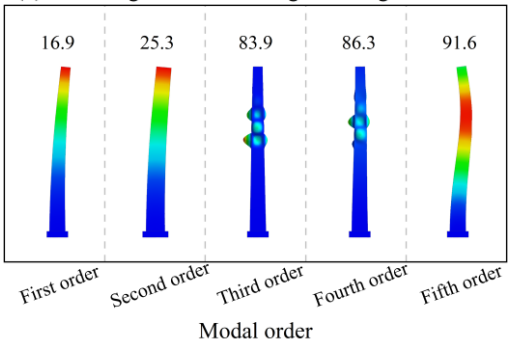

(b) Buckling mode under optimized conditions

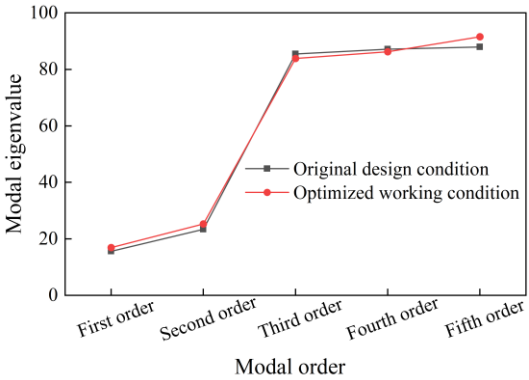

(c) Modal eigenvalue comparison

Fig. 9. Comparison of eigenvalues of buckling modes

Based on Fig. 9, it can be observed that the trend of eigenvalue variation with mode order for the optimized pier remains consistent with that of the original design pier. Additionally, the first two eigenvalues of the optimized pier are greater than those of the original design condition, and all buckling modes exhibit overall instability. Therefore, the proposed optimization scheme for the hollow thin-walled pier baffles in this study is feasible and more conducive to construction.

4 Conclusions

With the aid of Midas Civil and Midas FEA finite element software, a study was conducted on the effects of transverse and longitudinal baffle configurations on the stability of hollow thin-walled tall pier shafts under maximum cantilever stage pier top forces and wind loads. The following conclusions were drawn:

1) The horizontal diaphragms have a minor impact on the overall stability of hollow thin-walled piers, primarily affecting their local stability. Reducing the number of horizontal diaphragms appropriately can facilitate construction.

2) The vertical diaphragms also have a minor impact on the overall stability of hollow thin-walled piers, primarily affecting their local stability. The thickness of the vertical diaphragms can be added to the wall thickness to enhance the overall stability of the piers.

References

1. Shu, C. Z., Jia, X. J. (2016) Research on the setting of hollow thin-walled pier diaphragm. Chinese and Foreign Highways, 2016, 36 (6): 155-158. DOI: 10.14048/j.issn.1671-2579.2016.06.035.
2. Yang, Y.C., Wang, C.Y., Chen, H.C. (2022) Analysis of the Setting and Stability Calculation of Inner Diaphragms in Hollow Thin Wall High Piers. Highway, 2022, 67 (1): 217-220. https://link.cnki.net/urlid/11.1668.U.20220111.1033.072.

3. Yang, J.L., Pang, J.J. (2015) Analysis of local and overall stability of thin-walled hollow high piers. Industrial Construction, 2015, 45 (11): 122-125. DOI:10.13204/j.gyjz201511023.
4. Li, S.Y., Chen, Z.B., Zhou, H., et al. (2018) Experimental study on the stability of hollow thin-walled high piers without transverse partitions. Experimental Mechanics, 2018, 33 (5): 696-706. https://kns.cnki.net/KCMS/detail/detail.aspx?dbcode=CJFQ&dbname=CJFDLAST2018&filename=SYLX201805004.
5. Wang, G., Guo, Z.H., Huang, Y. (2020) Stability analysis of double limb thin-walled high piers without transverse partitions. Engineering and Construction, 2020, 34 (2): 294-297. https://kns.cnki.net/KCMS/detail/detail.aspx?dbcode=CJFQ&dbname=CJFDLAST2020&filename=GJDA202002043.
6. Li, Q.G., Liang, T.W., Liu, Z.Q. (2020) A study on the influence of diaphragm on the dynamic response of hollow thin-walled high pier bridges. Highway Transportation Technology, 2020, 37 (S2): 129-134. https://kns.cnki.net/KCMS/detail/detail.aspx?dbcode=CJFQ&dbname=CJFDLAST2021&filename=GLJK2020S2024.
7. Cheng, J.L. (2023) A study on the influence of vertical partitions on the stability and seismic resistance of low tower cable-stayed bridges with ultra-high piers. Chongqing Jiaotong University, 2023. DOI: 10.27671/d.cnki.gcjtc.2023.000350.
8. Zheng, B. (2017) Stability analysis of hollow thin-walled high piers and research on the method of setting transverse diaphragms. Wuhan University of Technology, 2017. https://kns.cnki.net/KCMS/detail/detail.aspx?dbcode=CMFD&dbname=CMFD201901&filename=1019806170.nh.
9. Mahmoud, M., (2010) Optimum Design of Cable-Stayed Bridges. The University of Western, 2010. https://ir.lib.uwo.ca/digitizedtheses/3213.
10. Wang, F., Tian, S.P., Zhuo, Y. (2012) Stability analysis of high pier and long span continuous rigid frame bridges. Journal of Railway Engineering, 2012, 29 (10): 57-62. https://kns.cnki.net/KCMS/detail/detail.aspx?dbcode=CJFQ&dbname=CJFD2012&filename=TDGC201210012.
11. Chen, H. (2011) Optimization design of hollow thin-walled high pier structure. Harbin Institute of Technology, 2011. https://kns.cnki.net/KCMS/detail/detail.aspx?dbcode=CMFD&dbname=CMFD2012&filename=1012003236.nh.
12. Tian, Z.J. (2013) Stability study on ultra wide circular end thin-walled hollow bridge piers. Lanzhou Jiaotong University, 2013. https://kns.cnki.net/KCMS/detail/detail.aspx?dbcode=CMFD&dbname=CMFD201401&filename=1013353033.nh.
13. Tang, F., Li, D.J. (2016) Stability and parameter influence analysis of high pier large-span continuous rigid frame bridges in mountainous areas. Journal of Railway Science and Engineering, 2016, 13 (3): 506-511. DOI: 10.19713/j.cnki.43-1423/u.2016.03.016.
14. Song, R.Y. (2023) Research on the arrangement of hollow thin-walled piers in continuous rigid frame bridges. Value Engineering, 2023, 42 (22): 72-74. https://kns.cnki.net/KCMS/detail/detail.aspx?dbcode=CJFQ&dbname=CJFDLAST2023&filename=JZGC202322023.
15. Granata, F.M., Longo, G., Recupero, A., et al. (2018) Construction sequence analysis of long-span cable-stayed bridges, 2018, 174 267-281. DOI: 10.1016/j.engstruct.2018.07.064.